

## AN ADAPTIVE REMESHING SCHEME FOR VORTEX DOMINATED FLOWS USING THREE-DIMENSIONAL UNSTRUCTURED GRIDS

Paresh Parikh  
ViGYAN, Inc.  
Hampton, Virginia

### SUMMARY

An adaptive remeshing procedure for vortex dominated flows is described, which uses three-dimensional unstructured grids. Surface grid adaptation is achieved using the static pressure as an adaptation parameter, while entropy is used in the field to accurately identify high vorticity regions. An emphasis has been placed in making the scheme as automatic as possible so that a minimum user interaction is required between remeshing cycles. Adapted flow solutions are obtained on two sharp-edged configurations at low speed, high angle-of-attack flow conditions. The results thus obtained are compared with fine grid CFD solutions and experimental data, and conclusions are drawn as to the efficiency of the adaptive procedure.

### INTRODUCTION

Mesh adaptation has been recognized as an efficient way to obtain accurate Computational Fluid Dynamic (CFD) solutions to complex flow problems. Adapting a mesh by placing more points in the region of dominating flow features (such as shocks, vortices etc.), increases the solution accuracy. The ability to automatically adapt a grid helps a user by not requiring him to have a knowledge of the location of the important flow regions in the field. As an example, for vortex dominated flows considered here, the locations of the origin of the vortices are usually known, but their trajectories in the field are not. For such a case, other than using a very fine grid everywhere, it would be extremely difficult to maintain a high grid resolution around the vortex core throughout the flow field.

Currently available mesh adaptation techniques can be classified into two broad categories: mesh movement and mesh enrichment. Mesh movement involves obtaining flow solution on an initial mesh, and at prescribed times in the solution process, moving mesh points towards the regions of important flow features. A major disadvantage of this procedure is that the accuracy of the final computation is limited by the number of points in the initial mesh. In mesh enrichment methods, starting from a relatively coarse mesh, a finer mesh is obtained either by introducing new points in the region of dominant flow features (refinement) or by generating a new mesh which is based on solution on the preceding mesh (remeshing). In the past all of these methods have been applied, to a varying degree of success, using both the structured and the unstructured meshes. A comprehensive review on this subject has appeared in a recent paper by Thompson et. al [1].

Unstructured grids are ideally suited for mesh refinement strategies, as the addition of points do not alter the data structure. However, this method has a shortcoming that the number of points increase rapidly with each refinement [2]. In the remeshing method, on the other hand, several new meshes are generated during advancement of the solution towards a steady state. A new mesh is based on the information from the previous flow solution. Since at each grid remeshing, finer meshes are produced in the regions of interest while they are coarsened in other regions, a good control is maintained on the total number of points while at the same time a good solution accuracy can be obtained.

---

\*Work done under NASA Contract No. NAS1-19672.

In the present paper, a solution adaptive remeshing technique for vortex dominated flows is demonstrated that couples a three-dimensional, unstructured mesh generator with an inviscid flow solver. An emphasis has been placed on developing an automated procedure that requires very little user interaction between remeshing cycles. In the section that follows, the grid generator, the flow solver and the adaptation strategy are discussed. This is followed by presentation of results on two sharp-edged configurations at flow conditions characterized by vortex domination. Finally, efficiency of the adaptation procedure is evaluated.

## PROCEDURE

The basic idea underlying any mesh adaptation scheme is to combine efficiently the mesh generation and the flow solver functions into a single procedure. The challenge is to integrate these functions in such a manner that the information produced by one is successively used by the other to ultimately generate a mesh which accurately resolves important flow features without using a large number of grid points. In the remeshing procedure described here, an advancing-front mesh generator (program VGRID) is integrated with an Euler equation solver (program USM3D) with an automatic procedure that produces input parameters for the mesh generator based on the solution on a previous grid. A similar study involving the same two programs was conducted for shock dominated, transonic flows, and was reported in Reference 3.

### Grid Generator

The advancing-front technique used in VGRID is a powerful tool for constructing tetrahedral meshes around complex configurations [4]. In this technique, the configuration of interest is represented by several surface patches. The grid element size is controlled by grid spacing parameters specified at the nodes of a secondary grid called the 'background grid'. The background grid is made up of a uniform Cartesian grid. Associated with the Cartesian grid is a number of 'point' and 'line' sources, at which the desired grid spacing parameters are specified. The spatial variation of these parameters in the field is determined by a process similar to that of computing the diffusion of heat from a number of discrete heat sources in a conducting medium. In addition to the symmetrical propagation of grid spacings, the program has the capability to specify directional propagation, thus giving the user uniform as well as directional control of grid spacing [5]. Thus, in VGRID the location, strength and directionality of the background grid sources need to be specified by the user. In the present adaptation strategy, these grid spacing parameters are automatically determined based on an earlier solution.

### Flow Solver

The flow solver used is an efficient Euler equation solver for unstructured tetrahedral cells. In USM3D, the spatial discretization is achieved by a cell centered finite-volume formulation using Roe's flux-difference splitting. A novel cell reconstruction process, which is based on an analytical formulation for computing solution gradients within tetrahedral cells, is used for higher order differencing. Solutions are advanced in time by a 3-stage Runge-Kutta time-stepping scheme with convergence accelerated to steady state by local time stepping and implicit residual smoothing. Recently the flow solver has been made more efficient by the use of a grid coloring scheme that has resulted in reduced CPU and memory requirements [6].

### Adaptation Procedure

In the adaptation method, the mesh generation and the flow solver functions are integrated into an unified procedure. A typical adaptive remeshing cycle is as follows. A coarse mesh is first generated on the configuration of interest. This first mesh is obtained by the user assigned 'first guess' for the spacing parameters, and is, usually, just fine enough to capture

approximate locations for vortices in the flow. Based on a partially converged flow solution on this mesh, spacing parameters are next calculated. The spacing parameters include location and strength of 'line' sources to be used in the background grid for the generation of the next mesh. This completes one adaptation cycle. As mesh is refined in the vicinity of vortices, and simultaneously coarsened in other areas of the flow, on successive meshes a more accurate representation of the flow is obtained. In practice several adaptation cycles are required to obtain a desired accuracy. The flow solution is allowed to converge fully on the final adapted grid.

### Adaptation Parameters

An important step in the present grid adaptation strategy is the calculation of the grid spacing parameters from a solution on the current mesh. These parameters are, in turn, used to generate a subsequent mesh. For the vortex dominated flows considered here, a finer mesh is needed in the vicinity of the vortices, and on the configuration surface along the vortex-induced suction peak. The task, then is to accurately find the location of the vortices in a three dimensional field. Once this is done, a finer mesh can be generated in and around these regions by placing 'line' sources in the background grid.

For vortex dominated flows, the core of the vortex can be successfully identified using entropy as the adaptation parameter [7]. Since an approximate location for the vortex origination is known (usually at the apex or kinks in the leading edge), one edge of the 'line' source is located there. The other end is found, by calculating entropy at all points in a user defined plane (search plane) downstream and tagging all the points at which the value of the adaptation parameter exceeds a specified threshold. The average of the coordinates for all such tagged points is then taken as the other end of the line source. The strength of the line source is taken as proportional to the value of entropy averaged over all the tagged points. To account for the variation in the strength and the location of the core, the line sources are placed in segments, instead of placing one long line source from apex to the end of the configuration and beyond. A similar procedure is followed for placing line sources on the surface along the vortex induced suction peak. The adaptation parameter used for the surface is the variation in 'static' pressure. The strength of the line source is inversely proportional to the value of static pressure.

The procedure described above has been automated so that the user only needs to specify approximate locations for the vortex origins and locations for the 'search planes' during the first cycle and threshold values for the adaptation parameters between remeshing cycles. All other required parameters are automatically calculated including creation of the input parameters for the next mesh. Once the location and the strength of the line sources are determined, a new mesh is generated, and a partially converged flow solution is obtained. This completes one remeshing cycle.

## RESULTS

The adaptation procedure described above has been applied to two vortex dominated cases, one with a single vortex and the other with multiple vortices. The adapted solutions thus obtained are compared with 'fine' grid CFD and experimental data for assessing the efficiency and accuracy, respectively of the adapted solutions. This section presents some of the results.

### Case 1: Hummel Delta Wing

The first case considered is that of a sharp-edged delta wing with an aspect ratio 1, known in the literature as 'Hummel' delta wing. The wing has a flat upper surface and a narrow triangular cross-section with a maximum thickness of 2.1 % of the chord located at 90 % root chord. The flow conditions selected are a  $M_\infty = 0.2$  and an angle-of-attack equal to  $20.5^\circ$ , in order to compare with the experimental data reported in Reference 8. At these conditions, there is a single pair of vortices emanating from the leading edge near the apex of the wing.

The adaptive remeshing scheme was tested beginning with a coarse grid (GRID 1) with 61,908 tetrahedra and 12,414 points. Of these 3,713 points represented the wing surface and the rest were field points. Based on a partially converged flow solution on this grid, an adapted grid was generated using the procedure described above. The adapted grid (GRID 2) had 287,652 tetrahedra, 53,380 total points and 8,344 surface points. The coarse grid solution was interpolated on the adapted grid and converged until the residuals were reduced by a 2.5 order of magnitude.

Figure 1 shows the effect of adaptation on the surface by comparing surface triangulation on the upper surface of both the unadapted and the adapted meshes. An increased mesh resolution on the surface under the vortex induced suction peak is clearly seen for the adapted case. Figure 2 shows the effect of adaptation on the field grid density by showing a slice through the grid at a plane normal to the wing, located at 70% of root chord. The higher mesh density in the region of vortex core is evident.

The efficiency of the adapted solution is established by comparing the adapted solution with an unadapted mesh which has fine resolution everywhere in the flow field. The 'fine' mesh was generated pretending limited *a priori* knowledge of the location of the vortex. This mesh has 412,567 tetrahedra and 76,865 points. Of these as many as 12,804 points represented the surface, thus giving a fine resolution on and near the surface.

Figure 3 shows a comparison of  $C_p$  at two locations on the wing, at 50% and 70% of root chord, respectively. Comparison is made between the adapted grid, the 'fine' grid and the experimental data. The adapted grid results agree closely with the 'fine' grid results. The computed inviscid results differ from the experimental (viscous) data in an expected manner [9]. The total CPU time for the adaptive cycle was 5,963 seconds on a Cray-YMP compared to 8,893 seconds for the 'fine' grid, which demonstrates the efficiency of the adaptive scheme.

#### Case 2: A MTVI Configuration

The next test case is a Modular Transonic Vortex Interactions (MTVI) wind tunnel model. It employs a 60° sharp-edged cropped delta wing with a segmented leading edge flap, and a chine shaped fuselage. Experimental data is available from a wind tunnel test conducted to investigate the interactions between the chine-forebody vortices and different vertical tail arrangements. The adaptive grid study was conducted for  $M_\infty = 0.4$  and  $\alpha = 10.54^\circ$ . This flow condition is characterized by the presence of multiple vortices.

For this case, computations were begun on a relatively coarse grid with 188,304 tetrahedral cells and 35,388 points (GRID 1). Two successively finer adapted grids were generated using the procedure described above. The final adapted grid (GRID 3) had 371,360 cells and 68,158 points.

Figure 4 shows a comparison of surface triangulation for the unadapted (GRID 1) and the adapted (GRID 3) cases. For the adapted case, clustering of the surface grid near leading edge as well as near the wing tip is evident representing the static pressure peak due to proximity of vortices to the configuration surface. Figure 5 shows a comparison of the field grid projected on to a cross sectional plane located at 93 % of root chord. Grid clustering around the vortex cores between the fuselage and the vertical tail and near the wing tip can be seen clearly. Finally, in figure 6 flow field results are compared between the unadapted grid, the adapted grid and experimental data. The  $C_p$  comparison is shown at a streamwise station located at 93 % of the root chord. In this figure, results are also compared from a 'fine' grid with 825,469 tetrahedra and 148,285 points [10]. During generation of the 'fine' grid, no special effort was made to cluster grid points around vortex core locations. A higher suction peak resulting from grid adaptation is evident. The fine grid did not capture the suction peak at the station shown due to lack of grid resolution there, while the adapted grid automatically provided the grid resolution needed. This case clearly establishes the ability of the adaptation procedure to automatically provide adequate grid resolution where needed. The whole adaptation cycle required about 2.5

hours of CPU time on a Cray-YMP computer, compared to about 4.0 hours for the 'fine' grid. The adapted results show a better accuracy with about 2.2 times less number of cells and about 38 % CPU saving compared to the 'fine' grid case.

### CONCLUSIONS

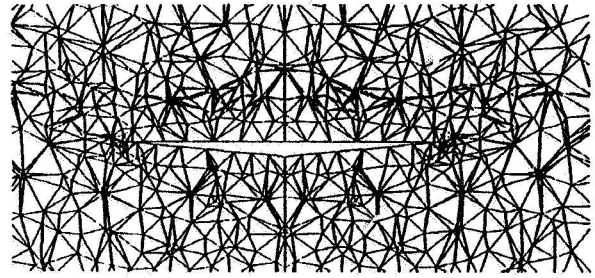
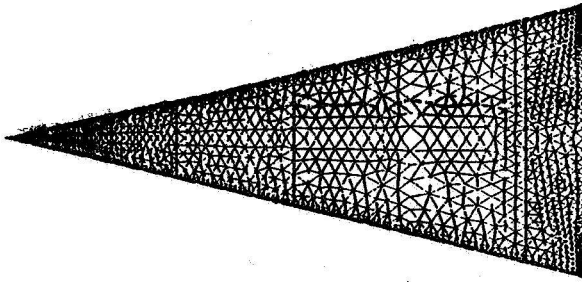
An automated adaptive remeshing scheme for vortex dominated flows is described. The procedure is shown to be an efficient technique for obtaining solutions especially when the locations of important flow features within the three dimensional flow field are not known. It is also shown that an adapted grid requires a smaller total number of grid elements compared to an unadapted grid, thus making the solution more amenable to a workstation environment.

### ACKNOWLEDGEMENTS

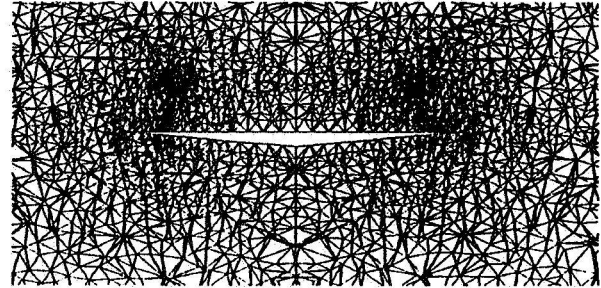
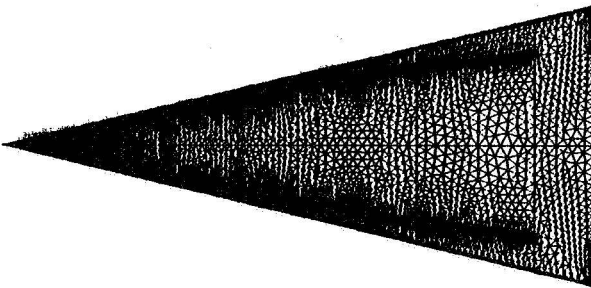
The work was supported under NASA Langley Research Center contract NAS1-19672 to ViGYAN, Inc. The author would like to thank Dr. Neal T. Frink, Transonic Supersonic Aerodynamics Branch and Dr. Shahyar Pirzadeh of ViGYAN, Inc. for many fruitful technical discussions. Thanks are also due to Mr. Brent L. Bates, ViGYAN, Inc. for MTVI fine grid solution.

### REFERENCES

1. Thompson, J.F.; and Weatherhill, N.P., Aspects of Numerical Grid generation: Current Science and Art. AIAA-93-3539-CP, August 1993.
2. Dannenhoffer III, J.F., A comparison of Adaptive Grid Redistribution and Embedding for Steady transonic Flows, *International Journal for Numerical Methods in Engineering*, Vol. 32, 1991, pp. 653-663.
3. Parikh, P.; and Frink, N.T., An Adaptive Remeshing Procedure for Three Dimensional Unstructured Grids, 4<sup>th</sup> International Symposium on Computational Fluid Dynamics, Davis, CA, September 1991.
4. Frink, N.T.; Parikh, P.; and Pirzadeh, S., Aerodynamic Analysis of Complex Configurations using Unstructured Grids, AIAA Paper 91-3292, 1991.
5. Pirzadeh, S., Structured Background Grids for Generation of Unstructured Grids by Advancing Front Method, *AIAA Journal*, Vol. 31, No. 2, February 1993, pp. 257-265.
6. Frink, N.T., Improvements to a Three Dimensional Unstructured Grid Flow Solver, AIAA Paper 94-0061, 1994.
7. Borsi, M., et al, Vortical Flow Simulation by using Structured and Unstructured Grids', In *Vortex Flow Aerodynamics*, AGARD-CP-494, Scheveningen, The Netherlands, October 1990.
8. Hummel, D., On the Vortex Formation over a Slender Wing at Large Angles of Incidence, AGARD-CP-247, Paper 15, 1978.
9. Ghaffari, F., On the Vortical-Flow Prediction Capability of an Unstructured-Grid Euler Solver, AIAA-94-0163, January 1994.
10. Bates, B. L., Private Communication.



UNADAPTED (GRID 1)



ADAPTED (GRID 2)

Figure 1: Surface Adaptation

Figure 2: Field Adaptation

..... Unadapted  
 ——— Adapted  
 ● Experimental  
 - - - - Fine

$$M_{\infty}=0.2, \alpha=20.5^{\circ}$$

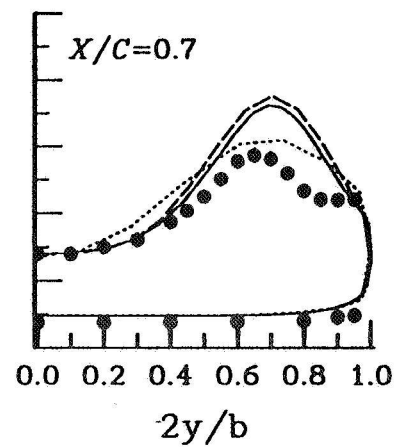
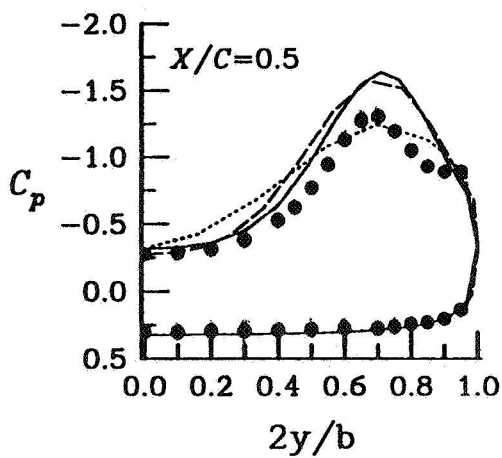


Figure 3: Comparison of Pressure Coefficient

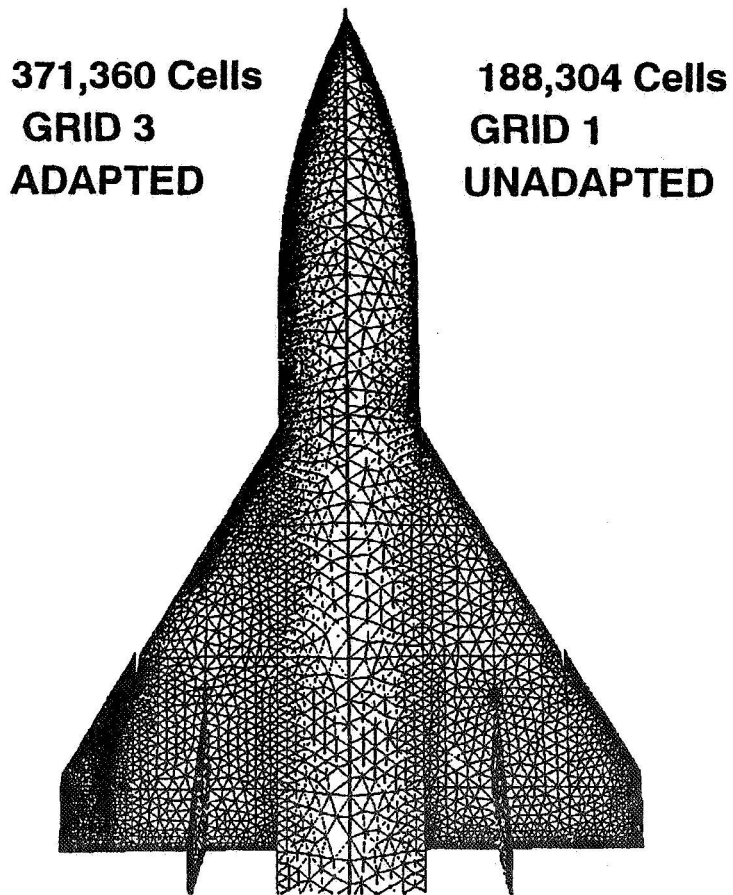


Figure 4: Surface Adaptation

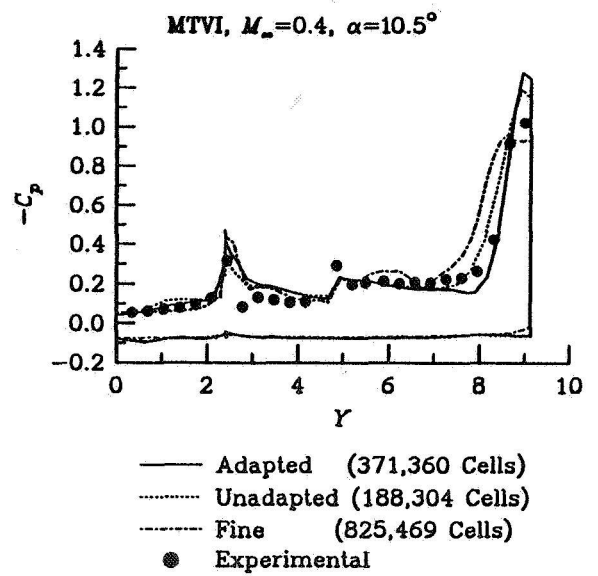


Figure 6: Comparison of Pressure Coefficient  
at  $X/C = 93\%$  Root Chord Location

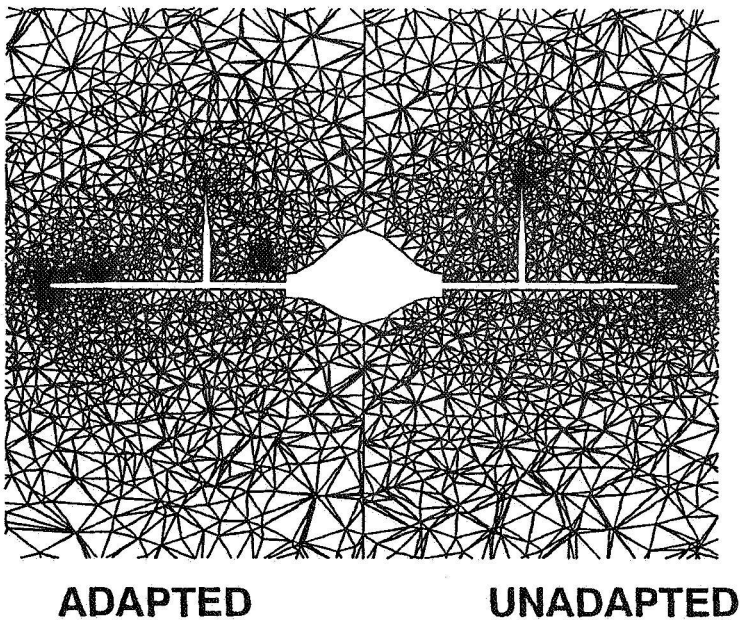


Figure 5: Field Adaptation